THE SHAPE OF CREEP CURVES IN NICKEL BASE SUPERALLOY C263

MAURIZIO MALDINI*, VALENTINO LUPINC, GIULIANO ANGELLA

The creep behaviour of the nickel base superalloy C263 has been studied at constant load and temperature in the 480–36 MPa/700–950 °C field. The shape of the creep curves has shown a very strong dependence on the applied stress. The experimental results have been rationalised supposing the mobile dislocation density increases during creep, from an initially low value at the beginning of the tests. With this hypothesis, the creep results have been modelled using two coupled differential equations, that have been successful in describing the creep behaviour in the entire explored stress/temperature field.

K e y w o r d s: Constitutive equations, creep, nickel base superalloy

TVAR CREEPOVÝCH KRIVIEK NIKLOVEJ SUPERZLIATINY C263

Študovali sme creepové správanie niklovej superzliatiny C263 pri konštantnom zaťažení v rozsahu od 480 do 36 MPa a v teplotnom intervale od 700 do 950 °C. Ukázalo sa, že tvar creepových kriviek výrazne závisí od aplikovaného napätia. Experimentálne výsledky sme vysvetlili na základe predpokladu, že hustota mobilných dislokácií sa zvyšuje v priebehu creepu z počiatočnej nízkej hodnoty na začiatku skúšky. Na základe tejto hypotézy a pomocou dvoch spojených diferenciálnych rovníc sa nám podarilo úspešne opísať creepové správanie v celom študovanom intervale aplikovaných napätí a teplôt.

1. Introduction

Stress-rupture and minimum creep rate properties cannot sufficiently define the creep properties of alloys utilised at high temperatures as the shape of the strain vs. time curves can considerably change with the applied stress. To take advantage of the modern engineering methods to design high temperature components, it is important to develop constitutive equations able to describe the whole creep curve. Moreover, since the number of load conditions in a component can be very large indeed, the constitutive equations must be able to extrapolate the creep curves for

CNR-IENI, Via Cozzi 53, 20125 Milano, Italy
* corresponding author, e-mail: maldini@ieni.cnr.it

all the requested load conditions from a reasonably limited amount of experimental data.

In the past most work has been done to describe, in terms of test parameters and microstructure, the first portion of the creep curves, i.e., the decelerating primary and the steady state or minimum creep rate. Less attention has been paid to the following accelerating creep, although this stage often dominates the creep curves of alloys utilised for high temperature applications.

The importance of describing the accelerating creep stage has been recognised more recently, and different phenomenological descriptions of accelerating creep behaviour have been proposed, some rationalised on strain basis [1, 2]:

$$\dot{\varepsilon} \propto \exp(a\varepsilon) \tag{1}$$

or

$$\dot{\varepsilon} \propto (1 + c\varepsilon), \tag{2}$$

some others have been rationalised on time basis [3], e.g.:

$$\dot{\varepsilon} \propto \exp(bt), \tag{3}$$

where ε and $\dot{\varepsilon}$ are strain and strain rate, respectively, while a, c and b are parameters generally depending on stress, σ, and temperature, T.

A totally empirical approach can be very attractive because of its simplicity, but its ability to predict creep behaviour for any arbitrary stress/temperature condition has been questioned, unless a very extensive experimental data base is utilised.

An alternative approach consists in using physical metallurgy knowledge to represent the strain rate in terms of variables ψ_i, governing the creep strain rate behaviour:

$$\dot{\varepsilon} = f(\sigma, T, \psi_1, \psi_2, \ldots, \psi_n) \tag{4}$$

and describe the evolution of these variables by the following set of differential equations:

$$\dot{\psi}_\mathrm{i} = g(\sigma, T, \psi_1, \psi_2, \ldots, \psi_n). \tag{5}$$

Examples of variables ψ_i are the density of mobile dislocations, their velocity and the interparticle spacing between the reinforcing particles.

The creep curves can be obtained integrating the coupled Eqs. (4) and (5).

This approach is apparently more complicated but the possibility of choosing a set of differential equations able to describe the actual creep and damage mechanisms operating in the material, appears very promising. In fact, although in

principle many creep mechanisms and damages can contribute to the creep strain rate, often most of them can be neglected and only one or two of them significantly influence the creep curve and must be modelled by Eq. (5) [4, 5]. Moreover, unlike the parameters of empirical equations, the parameters in Eqs. (4) and (5) are correlated with physical quantities that can suggest their stress and temperature dependence allowing confident extrapolations.

The aim of the present paper is to model the creep curve shape of C263, a polycrystalline Ni-base superalloy used in combustion chambers of aeroengines in the very wide stress/temperature field that the various parts of these components can experience during service, defining explicitly the differential Eqs. (4) and (5).

In this work we have neglected the initial very small and short decelerating primary creep and analysed the dominant accelerating stage after the minimum creep rate was attained. Ripening of the reinforcing particles during creep also has been neglected because it does not significantly affect the creep strain trajectory [4].

2. Material and experimental procedur

The material studied in this work is C263, a polycrystalline Ni-base superalloy used in combustion chambers of gas turbines. The nominal chemical composition of the alloy is given in Table 1. The heat treatment sequence is as follows: 2 h/1150 ℃ water quenching + 8 h/800 ℃ air cooling. The average grain size of the alloy is about 0.1 mm, the volume fraction of the reinforcing phase γ' at 800 ℃ is 10 %, the average γ' spheroid particle size is $\sim$ 22 nm. The γ' solvus temperature was measured around 920 ℃. Constant load tensile creep tests were run on cylindrical specimens in the stress/temperature field 480–36 MPa/700–950 ℃ producing rupture times in the 70–1250 h range. The creep specimens with cylindrical symmetry had 5.6 mm gauge diameter and 28 mm gauge length were machined out of 12 mm diameter bars. Creep strain was continuously monitored using capacitive transducers connected to extensometers clamped to the specimen shoulders. Three thermocouples were placed along the gauge length allowing controlling the temperature gradients. The furnace was controlled by the reading of the central thermocouple.

Table 1. Nominal chemical composition [wt.%] of Nimonic 263

Ni	Co	Cr	Mo	Ti	Fe	Mn	Al	Si	C
Bal.	20	20	5.8	2.1	0.7	0.6	0.45	0.4	0.06

Table 2. Nimonic 263 creep tests

Temperature [°C]	Nominal stress [MPa]	Time to rupture [h]	Creep strain to rupture, ε_{cr} [%]
700	480	74.0	2.4
	380	594.3	2.6
800	225	94.0	4.5
	180	270.8	3.6
	135	902.3	3.4
900	80	119.6	19
	70	254.7	19
	55	1254.1	13
950	50	77.5	60
	45	165.7	43
	36	492.9	40

3. Creep results

The experimental results, summarised in Table 2 and in Fig. 1, show the decelerating primary creep is always very small as often found also in other nickel base superalloys for stresses/temperatures relevant for applications. At the lowest explored stresses the decelerating stage can be hardly detected by an examination of the strain vs. time record. It becomes more pronounced at higher stresses, but its contribution to the creep curve is always modest: the creep strain due to the decelerating stage, is always smaller than the calculated elastic strain, σ/E, obtained during the initial loading.

In contrast, decreasing the applied stress the importance of the accelerating creep that follows the minimum creep rate becomes progressively more pronounced, and the shape of the creep curve strongly depends on the applied stress. In particular, in the 135–480 MPa/800–700 °C range, the accelerating creep exhibits a straight line in a plot strain rate vs. strain (Fig. 1c) and, consequently, in a plot log(strain rate) vs. time as it was found in many other γ' reinforced nickel base superalloys [2, 4].

In the tests at 900 and 950 °C, after the minimum creep rate is obtained, the rapidly accelerating stage follows, leading to a long steady-like state (Fig. 1d).

It is obvious that the first accelerating creep stage in the tests performed at 900 and 950 °C, i.e., the creep stage immediately following the minimum creep rate, can not be attributed to fracture mechanisms, since it leads to steady state. This behaviour suggests that the same mechanism is responsible for the accelerating creep detected in the tests at 700 and 800 °C, although in this case a contribution of fracture mechanisms, in particular intergranular cavitation, can not be excluded. Following Dyson and McLean [4] the accelerating creep has been mainly attributed to the multiplication of mobile dislocations.

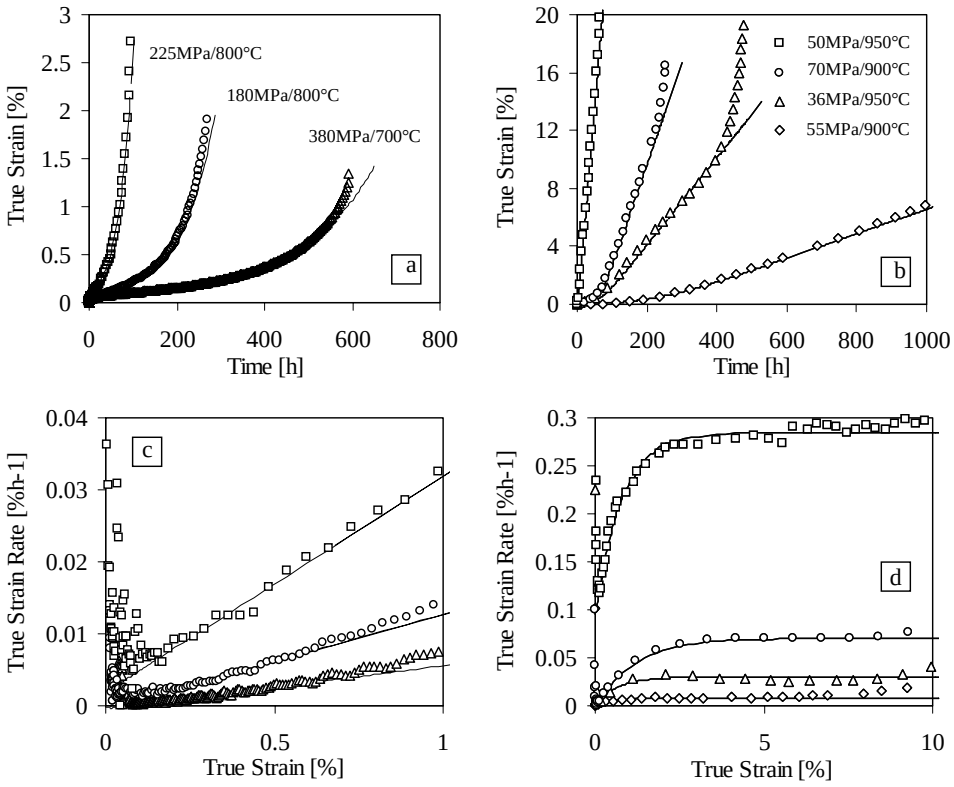

Fig. 1. A selection of strain vs. time creep curves performed at (a) 700/800 °C and (b) 900/950 °C. The same creep curves are replotted as strain rate vs. strain, respectively, in Figs. 1c and 1d. The accelerated creep curves are fitted using the equations obtained through the proposed model. The tests at 700–800 °C show a linear relationship between strain rate and strain. In the tests at 900–950 °C, the accelerating creep is followed by a steady state stage.

For all the test conditions, the final fracture is preceded by a short further accelerating stage, not reported in Figs. 1c,d.

It is important to note the strain to rupture for the creep tests strongly depends on the test conditions: it is 40–60 % in the tests at 950 °C, becoming as low as 2–5 % for the tests at 700 and 800 °C. Close examination of the creep strain to rupture behaviour of a similar C263 alloy at 800 °C appears in [6].

4. Creep strain constitutive model

The strain rate produced when a density ρ of mobile dislocations is moving at

a mean velocity v, is given by the Orowan relation:

$$\dot{\varepsilon} = b\rho v, \tag{6}$$

where b is the Burgers vector. This equation is the explicit form of Eq. (4). Creep constitutive equations can be determined combining Eq. (6) with evolution equations for ρ and v.

In general the creep strain rate depends on the volume fraction and inter-particle spacing of the reinforcing γ' particles, but it has been shown the coarsening of γ' particles *during* the creep test can contribute, but it is not the primary cause of the large and dominant accelerating creep stage, often detected in nickel base superalloys [4, 7, 8]. In fact a rapid accelerating creep, after the negligible initial decelerating creep, has been also detected in the tests performed at 950 ℃, above the γ' solvus temperature, when γ' is completely dissolved before the creep test is started.

The main mechanism responsible of the accelerating creep has been suggested to be the multiplication of mobile dislocations with strain [4, 8–10] according to the following relationship:

$$\dot{\rho} = \delta v \rho, \tag{7}$$

where δ is a constant.

To experimentally confirm the Eq. (7) can be questionable because transmission electron microscopy measurement of the mobile dislocation density in nickel base superalloys with large fraction of reinforcing phases can be very difficult, but the Eq. (7) is supported also by indirect experimental evidences, i.e.:

– Total dislocation density in nickel base superalloys tends to increase with strain during creep from an initial low value ρ° [11] at the start of the test.

– The combination of Eqs. (6) and (7) entails a linear relationship between strain rate and strain that has been experimentally observed during the dominant accelerating creep stage in many nickel base superalloys, as it is observed also in the C263 alloy in the creep tests at 700 and 800 ℃.

– Equation (7) seems to well describe the physics of creep, as, combined with Eq. (6), it has shown better capability of predicting creep behaviour in variable stress and temperature creep tests compared to empirical methods such as the strain hardening rule [12].

4.1 Evolution of mobile dislocation density during a creep test

Equation (7) assumes that the mobile dislocations multiply by a velocity-dependent process and neglects the contribution of the dislocation-dislocation interaction that reduces the dislocation density with a rate proportional to ρ^2 as

proposed by Johnston and Gilmann [13]. Ignoring the dislocation-dislocation interaction can be an acceptable simplification in the tests performed at 700 and 800 ℃, where the low initial density and the small strain to rupture keeps the dislocation density low during the whole test. Conversely Eq. (7) is an oversimplification for the tests at 900 and 950 ℃, where the large strain to rupture allows the dislocation density to increase during creep from an initial low value up to a density where dislocation interactions can not be neglected. In fact, TEM observations of C263 alloy crept specimens at 950 ℃, [8], show clearly the development of a dislocation network, that does not appear in the tests at 800 ℃.

The net change of mobile dislocation density is given by:

$$\dot{\rho} = \delta v \rho - h \rho^2, \tag{8}$$

where δ and h are constants [13]. If the dislocation density is low, the square term can be neglected and we obtain again Eq. (7). According to Eq. (8), the density of mobile dislocations evolves from an initial value ρ°, at the beginning of the test, to a steady state value $\rho_{ss} = \delta v/h > \rho^\circ$ when $\dot{\rho} = 0$ and, in parallel, the strain rate increases, from an initial low value, $\dot{\varepsilon}^\circ = \rho^\circ b v$, towards the steady state, $\dot{\varepsilon}_{ss} = \rho_{ss} b v$.

When fracture does not intervene early, e.g. in creep tests at 900–950 ℃, a stabilisation of the creep rate towards a steady state has been experimentally observed (Fig. 1d).

The Eq. (8) can also describe a decelerating transient regime when a large quantity of dislocations are present at the beginning of the creep test, resulting in $\rho^\circ > \delta v/h$. It is the case of the creep tests performed on austenitic steel when the applied creep stress is higher than the yield stress of the material. For example Li has used this equation to describe the primary creep of a stainless steel [14].

In general, the change of creep strain rate through the evolution of ρ can be described combining Eqs. (6) and (8). The equation set can be integrated to obtain ε vs. time [14] or the strain rate $\dot{\varepsilon}$ as a function of strain:

$$\dot{\varepsilon} = \dot{\varepsilon}_{ss} \left(1 - \frac{\dot{\varepsilon}_{ss} - \dot{\varepsilon}^\circ}{\dot{\varepsilon}_{ss}} \exp\left(-\frac{\delta v}{\dot{\varepsilon}_{ss}} \varepsilon \right) \right) \tag{9}$$

or time:

$$\dot{\varepsilon} = \dot{\varepsilon}_{ss} \left(1 - \frac{\dot{\varepsilon}^\circ - \dot{\varepsilon}_{ss}}{\dot{\varepsilon}^\circ} \exp(-\delta v t) \right)^{-1}. \tag{10}$$

For the tests performed at 700–800 ℃, Eq. (8) is reduced to Eq. (7) and the coupled equations describe a linear relationship between strain rate and the accumulated strain:

$$\dot{\varepsilon} = (\dot{\varepsilon}^\circ + \delta v \varepsilon) \tag{11}$$

and, consequently, an exponential dependence on time:

$$\dot{\varepsilon} = \dot{\varepsilon}^{\circ} \exp(\delta v t). \tag{12}$$

4.2 Evolution of mean dislocation velocity during a creep test

It is evident, from Eq. (6), that the value of the mean dislocation velocity, v, is important to determine the strain rate and then the time to rupture in a creep test. But the shape of the creep curves depends on the evolution, during creep, of both ρ and v. Here the mean dislocation velocity seems to play a secondary role: it explains the initial small decelerating creep in the tests characterised by a dominant accelerating creep (e.g. C263 at 700–800 ℃), sometimes followed by steady state creep (e.g. C263 at 900–950 ℃).

In fact the dislocation velocity is driven by an effective stress, i.e. the applied stress reduced by an internal stress. After the initial loading, as creep proceeds, the internal stress grows causing a reduction of mobile dislocation velocity producing at the beginning a short stage of strain deceleration. In the tests on C263 the small size of the decelerating creep ($\varepsilon_{\mathrm{d}} < \sigma/E$) suggests that the internal stress is due to a redistribution of stresses between different creep resistance regions of the material [15–16], for example between grains with different Schmid factor and, in turn, different creep resistance. At the end of the small decelerating primary creep, not modelled in this work, the redistribution of the stresses can be considered completed and both the internal stress and the dislocation velocity almost constant. The following accelerating strain stage is then attributed to a change in the mobile dislocation density.

Considering the mean dislocation velocity constant after the initial decelerating creep can be an acceptable simplification, especially in the tests performed at 700 and 800 ℃. In fact during the following accelerating creep no other long range internal stresses are built up due to, for instance, subgrain development. The mobile dislocation velocity is controlled by the average γ' particle distance (the dislocation links are always much longer than the particle interspacing), consequently the particle coarsening during the creep tests at 700 and 800 ℃ can modify the dislocation velocity, but this produces only a minor effect on accelerating the creep strain compared to the dislocation density evolution effect [4, 7, 8] and it has been neglected in this work.

No subgrain boundaries have been detected in crept specimens at 900 and 950 ℃, when very small or no volume fraction of γ' reinforces the alloy. For this reason, and in order to obtain simple constitutive equations, we have considered constant the mean dislocation velocity after the decelerating creep also at these high

temperatures. It is acknowledged that this is a simplification as the increment of the dislocation density during the accelerating creep, can produce a reduction in dislocation velocity contributing to reach the steady state stage after the rapid accelerating stage. Further experimental work is needed to refine the model in this regard.

5. Creep curve analysis

The authors have considered the evolution of the mobile dislocation density as the dominant process to describe the shape of the creep curves, and have ignored the effect of any dislocation velocity changes after the initial decelerating creep strain in order to obtain simple constitutive equations able to capture the essence of the material creep behaviour.

In the model there are three independent adjustable parameters:

$\dot{\varepsilon}_{ss}$ = steady state strain rate appearing when accelerating creep saturates,

$\dot{\varepsilon}^{\circ}$ = extrapolated strain rate at $t = 0$,

δv = parameter controlling the accelerating stage of creep.

In general the change of creep strain rate can be described combining Eqs. (6) and (8). For the tests at 700–800 ℃, when the experimental strain rates during the long accelerating creep show a linear relationship with the accumulated strain, Eq. (8) is reduced to Eq. (7). Figure 1 shows a comparison between a selection of experimental ε vs. time and $\dot{\varepsilon}$ vs. ε creep curves and the interpolation by the proposed equations. The good match between experimental data and the fit obtained by Eqs. (6) and (8) shows that the same set of equations can be utilised to describe the dominant stage of all the creep curves at the explored temperatures, i.e.: the accelerating creep at 700 and 800 ℃, that follows the minimum creep rate and the accelerating creep at 900–950 ℃ that follows the minimum creep rate and leads to the steady state. The small data base available does not allow to define reliable stress and temperature dependencies of the equation parameters to allow extrapolations to different stress and temperature test conditions. It is important to note that the same physical mechanisms producing the accelerating creep at 700–800 ℃, that appears as tertiary creep leading to fracture in this range, also produce the accelerating creep stage that leads to the steady state at 900–950 ℃. The main difference between the two behaviours is due to an early start of damage mechanisms leading to fracture after 2–5 % of strain at 700–800 ℃, while the damage mechanisms leading to fracture start to operate only after the steady state at 900–950 ℃, producing rupture elongations of 40–60 %.

6. Conclusions

The examined creep curves of C 263 consist mainly of accelerating and steady state creep. The minimum creep rate, appearing after the initial decelerating creep,

must not be confused with steady state creep. The steady state stage appears only in the tests run at 900–950 ℃ after the rapid accelerating creep. In the tests at 700–800 ℃, early fracture mechanisms interrupt the creep curve before the steady state is reached. At these temperatures the tertiary creep exhibits a linear relation between strain rate and strain.

The large accelerating stage detected in the tests at 950 ℃, when all the reinforcing γ' particles are dissolved in the matrix, confirms the assumption that the accelerating stage in this class of alloys is not due to the γ' particles coarsening, but, rather, to the dislocation density increase.

The constitutive equation based on evolution of mobile dislocation density, initially proposed by Li [9] to describe the primary creep in steels, has been shown to be able to describe the accelerating creep after minimum creep rate of the studied alloy.

Acknowledgements

This work has been performed within Brite Eu-Ram III CPLIFE project BRPR-4034 (1997–2001) supported by EC Bruxelles.

REFERENCES

[1] SANDSTRÖM, R.—KONDYR, A.: Mechanical Behaviour of Materials. Vol. 2. Oxford, Pergamon Press 1980.
[2] MALDINI, M.—LUPINC, V.: Scripta Metall., *22*, 1988, p. 1737.
[3] EVANS, R. W.—PARKER, J. D.—WILSHIRE, B.: In: Proceedings Recent Advances in Creep and Fracture of Engineering Materials and Structures. Eds.: Wilshire, B., Owen, D. R. J. Swansea, UK, Pineridge Press 1982, p. 135.
[4] DYSON, B. F.—MCLEAN, M.: Acta Metall., *31*, 1983, p. 17.
[5] ASBHY, M. F.—DYSON, B. F.: In: Proceeding Advances in Fracture Research. Eds.: Valluri, S. R. V. et al. Vol. 9. Pergamon Press 1984, p. 1.
[6] ZHANG, Y. H.—KNOWLES, D. M.: Mater. Sci. and Tech., *18*, 2002, p. 917.
[7] DYSON, B. F.—MCLEAN, M.: In: Proceeding of the IUTAM Symposium on Creep in Structures. Eds.: Murakami, S., Ohno, N. The Netherlands, Kluwer 2000, p. 3.
[8] MANONUKUL, A.—DUNNE, F. P. E.—KNOWLES, D.: Acta Mater., *50*, 2002, p. 2917.
[9] DYSON, B. F.: Rev. Phys. Appl., *23*, 1988, p. 605.
[10] GILMAN, J. J.: Micromechanics of Flow in Solids. New York, McGraw-Hill 1969.
[11] HENDERSON, P. J.: Scripta Metall., *22*, 1988, p. 1103.
[12] MALDINI, M.—LUPINC, V.: In: Proceeding 4th Inter. Conf. on Creep and Fracture of Engineering Materials and Structures. Eds.: Wilshire, B., Evans, R. W. London, The Institute of Metals 1990, p. 951.
[13] JOHNSTON, W. G.—GILMAN, J. J.: Appl. Phys., *30*, 1959, p. 129.
[14] LI, J. C. M.: Acta Metall., *11*, 1963, p. 1269.
[15] DYSON, B. F.: In: Proceeding Creep Behavior of Advanced Materials for the 21st Century. Eds.: Mishra, R. S. et al. Warrendale, Pennsylvania, TMS 1999, p. 3.
[16] ION, I. C.—BARBOSA, A.—ASHBY, M. F.—DYSON, B. F.—MCLEAN, M.: NPL Report, Teddington, DMA A115, 1986.

Received: 5.4.2004